Enabling low-cost and sustainable fuel cells

Frederic Jaouen

PHYSICAL SCIENCES/CHEMISTRY/CATALYSIS/ELECTROCATALYSIS [/639/638/77/886]
PHYSICAL SCIENCES/CHEMISTRY/ELECTROCHEMISTRY/FUEL CELLS [/639/638/161/893]
PHYSICAL SCIENCES/MATERIALS SCIENCE/MATERIALS FOR ENERGY AND CATALYSIS [/639/301/299]

FUEL CELLS

Enabling low-cost and sustainable fuel cells

A hydroxide exchange membrane fuel cell is demonstrated that uses a nickel-based anode and a cobalt-manganese-oxide cathode to achieve a power density of 488 mW cm^{-2} at 95°C.

Frédéric Jaouen

While fossil fuels currently fulfil our energy needs, renewable energies will play an increasing role. Green hydrogen could be produced at scale from renewable electricity and back-converted to electricity on demand in fuel cells. Polymer-electrolyte fuel cells are well-suited for automotive and other applications requiring a quick start. Owing to its high pH environment, the hydroxide exchange membrane fuel cell (HEMFC) holds promise to work efficiently with electrocatalysts based on abundant and cheap chemical elements.[1] While several Fe-N-C cathode catalysts recently demonstrated high performance in HEMFC, [2-3] developing active anode catalysts for the hydrogen oxidation reaction (HOR) without platinum group metals (PGM) remains a challenge.[4-5]

Now, writing in Nature Materials, Weiyan Ni and co-workers report how nickel nanoparticles can be made highly active towards HOR in high-pH electrolyte. They demonstrated a peak power of ca 450 $W \cdot cm^{-2}$ at 80°C with a H_2/O_2 HEMFC comprising their optimized Ni-based anode catalyst paired with a Co-Mn-O_x cathode catalyst (Figure 1a).[6] The highest peak power reported previously for a HEMFC at 80°C with a PGM-free anode was ca 350 $mW \cdot cm^{-2}$, but achieved with a PGM-based cathode (Figure 1b).[7] The highest peak power reported hitherto on PGM-free HEMFCs was circa 80 $mW \cdot cm^{-2}$,[8], highlighting the size of step forward achieved by Ni and co-workers.

Metallic nickel nanoparticles embedded in a nitrogen-doped carbon matrix were prepared via annealing at 390°C in reducing atmosphere a metal-organic-framework (MOF) comprised of Ni^{2+} cations and benzenetricarboxylate ligands (btc), $Ni_3(btc)_2$. The highest HOR activity was obtained with a H_2:NH_3:N_2 annealing atmosphere. NH_3 was key to nitrogen dope the carbon-phase derived from organic ligands, as well as minimizing the size of nickel particles. H_2 combined with NH_3 was necessary to increase graphitization and so electron-conductivity of the carbon-phase obtained by annealing $Ni_3(btc)_2$ (Figure 2a). Transmission electron microscopy images of the optimized catalyst (Ni-H_2-NH_3) revealed separated zero-valence nickel nanoparticles of ca 13 nm size embedded in a carbon matrix (Figure 1c). The authors demonstrated with surface-sensitive techniques that an electronic interaction takes place between the N-doped carbon matrix and nickel nanoparticles, this interaction being likely magnified by the extended interface between the nickel nanoparticles and the N-C matrix (solid blue lines in Figure 1c). Ultraviolet photon spectroscopy in particular, showed weakened adsorption strength for the three materials derived from $Ni_3(btc)_2$ relative to a metallic nickel reference. The catalyst morphology and composition (ca 83 wt % Ni, remainder C and N) are also different compared to the previous best Ni-based HOR catalyst, comprised of NiCu alloy nanoparticles supported on undoped carbon (ca 13 wt% Ni, 1.5 wt% Cu and 86 wt% C) (Figure 1d).

After normalisation to electrochemically-accessible nickel surface area, the HOR activity of Ni-H_2-NH_3 was ca 2.5 times higher than the most active Ni-based HOR catalyst reported hitherto.[9] Modification of the electronic state of nickel by interaction with the N-C shell seems to play an important role in tuning hydrogen- and hydroxyl-binding energies on nickel, which certainly partly explains the high HOR activity observed (Figure 2b).

Other phenomena may however need to be invoked to account for the improved HOR activity of nickel in this material. Since the nickel nanoparticles seem fully covered by a N-C shell of typically 2-3 nm (Figure 1c, Figure 2b-c) and the electrochemically-measured surface area of nickel is commensurate with that expected for spherical nanoparticles of average diameter 13 nm, this implies that the N-C shells are porous, allowing the passage of H_2, OH^- and H_2O species (Figure 2b-c). The nickel surface is therefore accessible to electrolyte and reagents, while having a substantial density of electrical junctions with the N-C shell (Figure 2c). The electronic percolation path throughout the catalyst powder seems to be secured by the N-C shells, as supported by the low electronic conductivity of the $Ni_3(btc)_2$ MOF annealed in N_2/NH_3. A morphology similar to that of Ni-H_2-NH_3 was observed, but the N-C phase was more disordered, leading to a ca 10x lower electronic conductivity relative to Ni-H_2-NH_3.

The peculiar architecture of the nickel/N-C/electrolyte interface achieved by W. Ni et al therefore may have triggered unusual physicochemical phenomena. First, if the pores in the N-C shell are sufficiently small (nanometre range), this could lead to confinement effects, decreasing the solvation shell of hydroxyl anions by a non-negligible interaction between ions or water molecules and pore walls. It is well-established, for example, that decreased solvation of ions in

nanoporous carbon materials leads to increased electrochemical capacitance.[10] The cavities existing in pristine $Ni_3(btc)_2$ MOF (5 and 9 Å, [11]) may well have been transferred to the N-C shells derived from its annealing at 390°C. Second, the presence of many junctions between N-C shells and the metallic nickel interface (Figure 2c) may support the so-called bifunctional mechanism for HOR, wherein some sites promote H_2 dissociation into two adsorbed hydrogen atoms while other sites bind hydroxyl anions, these combined features being desired to carry out the HOR (Eq. 1).

$$H_2 + 2OH^- \Rightarrow 2H_2O + 2e^- \qquad (1)$$

Encapsulation of metallic nickel nanoparticles by a thin but nanoporous shell of nitrogen-doped conductive carbon may therefore be at the root of the high performance. In a broader sense, some analogy can be drawn with the recently reported modified selectivity of metallic platinum when it is covered by an overlayer of porous TiO_x.[12] The improved selectivity for HOR relative to dioxygen electro-reduction reaction of Pt@TiO_x vs. bare Pt was tentatively assigned to a sieving effect due to the pore network of the TiO_x overlayer. The preparation of porous shells with tunable and well-controlled pore size is generally desirable for improved understanding and optimized activity or selectivity of such materials. Indeed, a set of materials with varying (controlled) pore sizes could unambiguously demonstrate the validity of any solvation shell effects, with no effect expected above a certain pore size.

The preparation by design of core@porous-shell materials could therefore find promising applications in electrocatalysis, enabling low-cost catalysts and further improvements in the activity, selectivity and/or stability of PGM-based catalysts. The work by Ni and colleagues certainly suggests that this would be a fruitful area of research.

Affilliation: Institut Charles Gerhardt Montpellier
CNRS – Univ. Montpellier – ENSCM
Montpellier, France
e-mail: frederic.jaouen@umontpellier.fr

References:

1. Adabi, H., Mustain, W. E. *ACS Catal.* **10**, 225-234 (2020).
2. Adabi, H. et al, *Nature Energy* **6**, 834-843, (2021).
3. Adabi, H. et al, *Materials Today Advances* **12**, 100179 (2021).
4. Oshchepkov A. G. et al, *ACS Catal.* **10**, 7043-7068 (2020).
5. Davydova, E.S. et al, *ACS Catalysis* **8**, 6665-6690 (2018).
6. Ni, W. et al, *Nature Materials* **21**, XXX (2022).
7. Roy, A. et al. *Sustainable Energy & Fuels* **2** 2268-2275 (2018).
8. Gu, S. et al. *Chem. Commun.* **49**, 131-133 (2013).
9. Ni, W. et al. *Angew Chem. Int. Ed.* **59**, 10797-10801 (2020).
10. Simon, P. *Chemical Society Reviews* **49**, 3005-3039 (2020).
11. Maniam, P. and Stock, N. *Inorg. Chem.* **50**, 5085-5097 (2011).
12. Stühmeier, B.M. et al. *ACS Appl. Energy Mater.* **2**, 5534-5539 (2019).

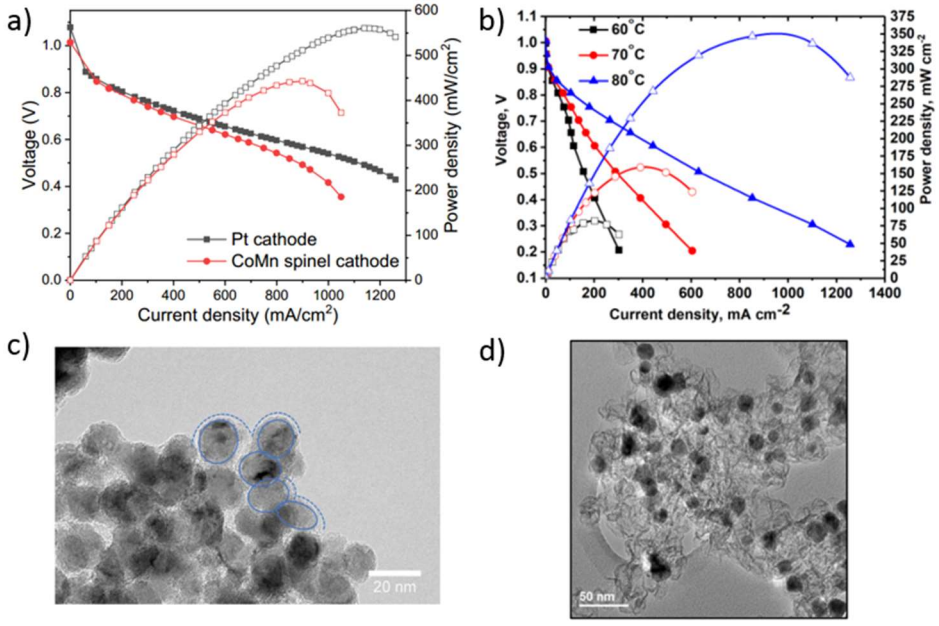

Figure 1 | Fuel cell performance and morphology of nickel anode catalysts. HEMFC polarisation curves at 80°C, **a**, with the Ni-H_2-NH_3 and a Co-Mn-O_x spinel cathode or a Pt/C cathode,[6] and **b,** previous achievement with a NiCu/C anode and a Pd/C cathode.[7] TEM image of **c,** Ni-H_2-NH_3,[6] and **d,** NiCu/C.[7] For both **a,** and **b,** pure H_2 and O_2 gas were fed at anode and cathode side, respectively. Figure 1b and 1d reproduced from Ref. 7 with permission from the Royal Society of Chemistry.

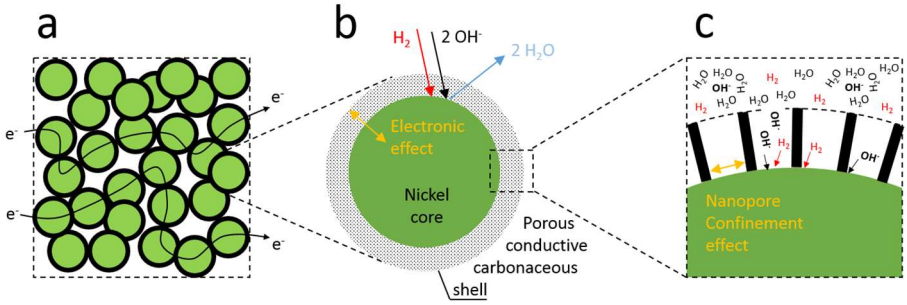

Figure 2 | Schemes of the nickel anode catalyst from [6] at different scales. **a**, nickel nanoparticles with a carbonaceous shell, requiring sufficient electronic conductivity of the shell, **b**, a single nickel-core and porous carbon-shell particle, here denoted by the grey coating, **c**, possible modified solvation shell of OH^- in idealised nanopores. **[Note to the art editor: Figure 1a taken from Figure S28 of reference 6. Figure 1b taken from Figure 6 of reference 7. Figure 1c taken from Figure S5 of reference 6, Figure 1d taken from Figure 1a of reference 7.**

Figure 2b, the grey coating on the sphere should look porous, i.e. there should be spaces from the surface to the surface of the green sphere. This could be represented by a half-filled shell as here. Figure 2c, if possible, it would be good if the black bars representing the pore walls are not straight.]

The authors declare the following competing interests:

The author declares no competing interests.